

## RESEARCH ARTICLE

# Line-Start Synchronous Reluctance Motor: A Reduced Manufacturing Cost Avenue to Achieve IE4 Efficiency Class

MARCO VILLANI<sup>1</sup>, GIUSEPPE FABRI<sup>1</sup>, (Member, IEEE), ANDREA CREDO<sup>1</sup>, LINO DI LEONARDO<sup>1</sup>, AND FRANCESCO PARASILITI COLLAZZO<sup>1</sup>

Department of Industrial and Information Engineering and Economics, University of L'Aquila, 67100 L'Aquila, Italy

Corresponding author: Marco Villani (marco.villani@univaq.it)

**ABSTRACT** The paper presents the Line Start Synchronous Reluctance Motor (LSSynRM) technology as a promising avenue to bring IE3 motor portfolios to the IE4 efficiency class at contained manufacturing costs. Indeed, the achieving of IE4 efficiency class is concerning many motor manufacturers, where the small-medium manufacturers seem to face the higher efforts in converting their product portfolio. To this extent, a methodology to improve the IE3 Induction Motor (IM) efficiency by introducing the Line Start Synchronous Reluctance motor technology in the IM motor is presented. The new motor design guidelines and constraints are figured out to reduce the impact on the manufacturing process. The paper presents a detailed experimental validation of the realized prototype in steady-state and transient operation referring to a target IE3 IM. The prototype proved to be a cost-effective, mass production-ready solution for super-premium efficiency IE4 motors. The LSSynRM technology demonstrated to be an effective high-efficiency avenue at reduced manufacturing costs in a broad panorama of low-inertia industrial applications.

**INDEX TERMS** Breakdown torque, comparison, critical inertia, direct-on-line, geared motor, IE4 efficiency class, induction motor, line-start, pull-in torque, starting transient, synchronous reluctance motor.

## I. INTRODUCTION

The worldwide growing demand for energy, and the problems of scarcity of sustainable sources, stimulated in the industry of electric motors international directives for the introduction of Minimum Efficiency Performance Standards (MEPS) and the related efficiency class IE1 (Standard-Efficiency), IE2 (High-Efficiency), IE3 (Premium-Efficiency), IE4 (Super Premium-Efficiency) [1], [2].

The MEPS mainly impact the Induction Motors (IMs) market, the widely used machine in industrial fixed speed applications. IM designers are pushing the technology towards its boundaries to comply with MEPS, increasing the cost of the motors by adopting higher quantity and quality of the active materials or by introducing new manufacturing processes [3].

The associate editor coordinating the review of this manuscript and approving it for publication was Feifei Bu<sup>1</sup>.

Costs are the main barrier that prevents the diffusion of IE4 motors; therefore, while policymakers register the low market share of IE3 solutions, manufacturers are concerned about which could be a cost-effective avenue to comply with the highest efficiency classes (IE4 and IE5) [3], [4].

Engaged by this context, designers are proposing, as a potential turnaround, a shift from the consolidated IM technology toward more efficient synchronous motor technologies with line-starting capabilities (direct-on-line starting motors) [4], [5], [6].

Recently, the Line-start Synchronous Reluctance Motor (LSSynRM) technology [7], [8] seems promising since it potentially exhibits high efficiency. Moreover, starting capabilities and power factor are being improved to adequate levels [9], [10], [11], [12], [13], [14], mitigating losses in cables and transformers.

Nevertheless, the required investments for the conversion of IMs manufacturing process and tooling seem still out

of the possibilities of many Small Medium Manufacturers (SMMs).

This paper presents how the LSSynRM is not only viable technology for high-efficiency motors, but it can be designed to be manufactured by using the same materials and most of the existing manufacturing processes adopted for an IE3 IM, allowing SMMs to offer an IE4 motor portfolio with reduced investments.

The paper starts by discussing the motivation, the advantages, and the drawbacks concerning the potential introduction of LSSynRM as a reference technology for high-efficiency motors in constant speed applications (Section II).

Section III recalls the operating principles at the base of the LSSynRM and reports the design guidelines and technical considerations. Then, the potentialities of the proposed technology are discussed in section IV based on specific tests carried out on the prototype.

Steady-state and dynamic experimental tests validate the LSSynRM acceptable capabilities compared with the reference IE3 IM and manufactured with the same tools and materials.

## II. HIGH-EFFICIENCY MOTORS: CONSIDERATIONS ON MANUFACTURING COST

The release on the market of a new motor portfolio involves several activities concerning the manufacturing process. The main motor manufacturing aspects are resumed in the following macro-areas:

- Raw material supply chain (electrical steel, enameled copper wires, rotor bars alloy, PM);
- Parts supply-chain: (shaft, bearings, housings, fans);
- Production and assembly: (lines and tooling, punches and die-cast molds);
- Validation and qualification: (new materials, parts, tools, and processes).

New product development represents a considerable effort for SMMs, especially in those cases where field tests support the product validation, eventually in cooperation with customers, or where the manufacturing process and the supply chain are certified for special applications, special environmental regulations, or specific customer needs.

Therefore, the first envisioned action to make the product portfolio compliant with the MEPS was the increase in the quantity and quality of active materials, causing an increase in the volume, weight, and cost of the electric motors. The efficiency was increased, but other performances of the IMs were degraded (e.g., reduced power factor and higher starting current) [15].

Hence, replacing the aluminum rotor with a copper rotor was also investigated to reduce cage losses in IMs. Still, the complex die-cast process and the material cost were evaluated as not affordable by a large part of the manufacturers [16].

Moreover, different no-tooling cost techniques to achieve MEPS are still investigated, but they seem limited in improving the IM efficiency at acceptable costs [17], [18].

Meanwhile, VSDs are being successfully adopted when more energy-efficient operations are achievable through variable speed operations. Nevertheless, in many fixed-speed (and load) applications, they are still undesired due to higher purchasing, commissioning, and maintenance costs more than the losses they introduce [19].

Recently, the Line-Start Synchronous Motor technology has been investigated due to its promising performance in terms of efficiency. Indeed, the operation at synchronous speed theoretically avoids slip losses in the cage, which usually represents about 20-30% of the overall loss of IMs [20].

Therefore, motor designers are proposing solutions based on PM or reluctance synchronous motor technology combined with a squirrel cage for the line starting capabilities, namely Line Start Permanent Magnet Synchronous Machines (LSPMMs) [21], [22], [23], [24] or Line-start Synchronous Reluctance Machines (LSSynRM) [7] [9], [10], [11], [12], [13], [14], [25], [26].

However, Line Start Synchronous motor is a new motor technology that implies a deep review of the manufacturing process and may expose SMMs to high investments.

Hence, to clarify the relationship between design upgrade, efficiency enhancement, and impact on materials and processes, the authors outlined Table 1, where the main design upgrades in terms of efficiency enhancement are reported along with the expected effects on material costs and manufacturing process.

While the impact on the manufacturing process of a motor design upgrade and the related efficiency enhancement needs to be accurately evaluated case by case, from the considerations reported in Table 1, it seems clear that each specific design upgrade is accounted to give low to medium benefits on motor efficiency. In contrast, it could highly impact the cost structure of the SMM. The exceptions are the design upgrades at the rotor level only if the rotor diameter and the die-cast process are not affected.

SPMMs or LSSynRM become suitable technology if achievable by the only rotor upgrade, with preference to the LSSynRM, which avoids PM costs and related supply chain and insertion process.

The possibility to convert an IE3 IM into an IE4 LSSynRM with low tooling cost, hence by upgrading mainly the rotor geometry, is investigated in this paper. A reference IE3 IM motor has been selected in cooperation with an SMM. The machine sizes and materials have been imposed as design constraints to reduce as much as possible the updates in the manufacturing process; Table 2 reports the main data of the reference IM designed for gear motor application but not limited to it.

About the bill of material, the M470-50A electrical steel of the IM is still adopted, along with the same copper wire and

**TABLE 1. IM design upgrade: impact on efficiency, materials, and manufacturing process.**

IE3 IM Design Upgrade	Impact on Efficiency	Impact on Material costs	Impact on Manufacturing Process
New Stator windings layout	Low	Low	<u>Minor to medium</u> -winding machine tuning or machine replacement
New wire size	Low	Low	<u>Minor</u> -winding machine tuning -supply chain and quality assessment
New Stator geometry	Low	None	<u>Medium</u> -new punch needed
New Stator outer diameter	Medium	Low - medium	<u>High</u> -new punch needed -new housing needed
New Stack length	Low to medium	Low to medium	<u>High</u> -(if new housing is needed)
New Rotor geometry	Medium	None	<u>Minor to medium</u> -new punch is needed, -Die-cast process to be assessed
Adoption of PM in the rotor	Medium	High	<u>Medium</u> - Cost of the magnets, - dedicated supply chain, - quality assessment, - insertion process
New End-rings	Low	Low	<u>Minor</u> -new die-cast mold, -die-cast process to be assessed
New rotor outer Diameter (same stator outer diameter)	Medium	Low	<u>Very high</u> -New rotor punch needed -New stator punch needed -New die-casting tools
New low losses electrical steel	Low	Medium	<u>Low to medium</u> -new supply chain and quality assessment
New bearings	Low	Low	<u>Low</u> -supply chain and quality assessment
New fan	Low	Low	<u>Low</u> -supply chain and quality assessment

the aluminum alloy for the die-cast rotor cage, the shaft, the bearings, the fan, and the housing.

**III. IM TO LSSynRM CONVERSION: DESIGN NOTES OF THE ROTOR GEOMETRY**

In detail, the LSSynRM can be thought of as a hybrid between an IM and a Synchronous Reluctance Motor (SynRelM) [8]; the squirrel cage is embedded inside the rotor core, and it has the only purpose of starting the motor, bringing it to work at synchronous speed.

At synchronous speed, the effect of the rotor squirrel cage is neglectable, and the rotor operates as in a SynRelM, achieving high efficiency as the cage losses are also neglectable. Since the cage slightly affects the SynRelM operations, the embedding of the rotor bars within the flux barriers is a consolidated design technique for LSSynRM [27]. A general layout of the LSSynRM rotor is detailed in Fig. 1, where some

**TABLE 2. Reference IE3 IM motor data.**

Rated power	kW	4
Line voltage	V	400
Frequency	50	50
Rated speed	Rpm	1450
Rated torque	Nm	25.5
Efficiency class		IE3
Rated efficiency	%	88.8
Frame size		IEC 112
Number of stator slots		48
Max. stack length	mm	180
Electrical steel		M470-50A
Rotor cage		die-cast Al
Stator outer diameter	mm	170
Stator inner diameter	mm	103
Airgap	mm	0.30
Slot fill factor		0.43
Motor weight (active parts)	Kg	30.1

flux barriers host a cage slot, obtained by designing an inner rib in the barrier.

Based on these concepts, the torque characteristic of the LSSynRM has been idealized, as shown in Fig. 2 [8]. The mechanical characteristics of the IM and SynRelM mesh through the so-called “pull-in” torque, ideally identifying the torque component that literally pulls the rotor from the asynchronous characteristics to the synchronous one. The starting torque, the pull-up torque, and the maximum torque have the same meaning as in a conventional IM. In contrast, the breakdown torque is the maximum torque the machine exhibit at synchronous operation [5].

To develop low tooling cost alternative to the target IM, its main torque components related to the start-up performance (i.e., starting torque, pull-up torque, maximum torque) become targets for the LSSynRM design steps. A rule of thumb about the breakdown torque at synchronous operation is to select the double of the IM rated torque as a target value. This condition assures an effective synchronous operation in case of spikes in the load torque and gives advantages in the pull-in step.

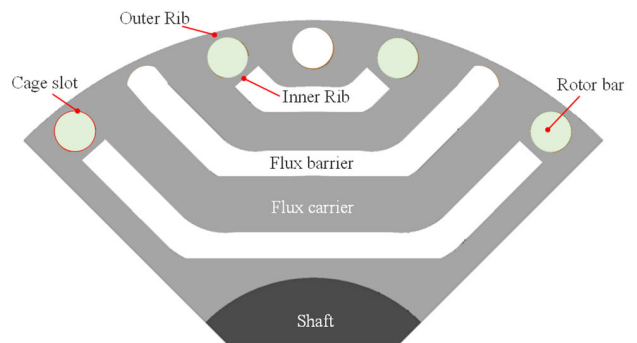


**FIGURE 1. Sketch of the LSSynRM rotor geometry in a four poles motor, three flux barriers, and symmetric cage.**

The term pull-in torque ideally identifies the torque that pulls the motor out of the asynchronous operating mode into the synchronous operating mode. It is difficult to be computed as it depends on the cage and reluctance torque

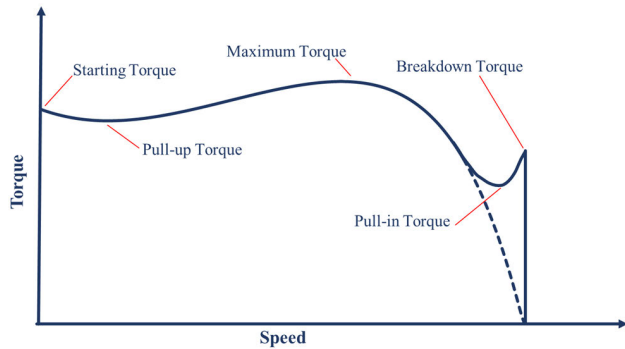


**FIGURE 2.** Average torque vs. speed characteristic of an LSSynRM.

contributions, and it is of minor relevance in evaluating the starting performance. Conversely, it is meaningful to consider the energy provided during the pull-in step and converted into kinetic energy, so the design constraints on the critical inertia become explicit [28], [29].

Exceeding the critical inertia has the result that the kinetic energy acquired by the rotor during start-up is not enough to sustain the “jump” at synchronous speed properly. For this reason, it is mandatory to ensure that the rotor has a reasonable acceleration during the starting transient: this can be achieved mainly by an improvement of the asynchronous characteristics.

To simplify the preliminary design of the rotor geometry, two main steps are envisioned: the design of the reluctance rotor and the design of the embedded squirrel cage. Indeed, reluctance contribution is relevant at the synchronous speed where the effect of the rotor squirrel cage is neglectable. Conversely, the squirrel cage works in starting operations where the reluctance contribution provides torque pulses.

The design of the rotor geometry for synchronous operations can be carried out in accordance with the best-practice design rules and procedures of SynRelM, particularly those related to the containment of the torque ripple [30], [31], [32]. Electrical steel, stack length shaft diameter, and outer rotor diameters are the same as the IM to pursue the low tooling cost approach. The number of slots of the available stator (48 slots) and the rotor diameter suggest the adoption of four flux barriers in the rotor core.

Nevertheless, the presence of the cage slots in the flux barriers introduces additional constraints in the barrier width to allow an effective die casting process. In the low tooling cost approach, the minimum width of the flux barrier should be selected according to the old IM bars' width not to affect the die-casting process. This choice allows for minimizing the assessment of the die-casting for the new rotor. Larger bars are not a concern from the die-casting point of view, giving the designer some flexibility.

Moreover, the introduction of the cage slot in the flux barriers suggests the adoption of a rectangular barrier shape among the most used ones (rectangular, circular, Fluid

Shape-Joukowski [8]). Indeed, rectangular barriers have a more regular shape close to the region of the cage slot, with a quasi-radial layout allowing for a better fitting of the rotor slots in the case of rectangular bars.

With the above considerations, the flux barriers can be shaped and optimized while performance at synchronous speed is evaluated. The optimized flux barriers of the LSSyn-RelM are shown in Fig. 3, where a symmetrical cage with round bars is envisioned at this step [33].

To improve the design of the rotor squirrel cage, the following consideration can be outlined:

- the end-rings should be the same as the IM to lower tooling costs.
- the rotor bars are constrained within the optimized flux barriers; (thickness of the flux barriers design has been already constrained to allow for die-casting of the rotor bars).
- deep rectangular bars are preferred to enhance the starting torque and increase the gradient of the asynchronous mechanical characteristics in the pull-in region. High-gradient asynchronous torque characteristics in the pull-in region facilitate the pull-in by bringing the rotor closer to the synchronous speed [34], [35].
- Moving the inner ribs far from the tangential ribs leads to improved reluctance performance.

The introduction of deep rectangular bars within the optimized flux barrier leads to an asymmetric rotor cage due to the non-radial layout of the rectangular flux barriers (Fig. 4). Moreover, the bars located in the fourth flux barrier are too close to be realized in a proper rectangular shape; hence, a potential simplification of the layout by adopting a unique single bar is proposed, as shown in Fig. 5. Thus, the fourth flux barrier is reshaped in a trapezoid to obtain a larger trapezoid bar slot. This tip widens the bar section in the region of the fourth flux barrier and reduces the equivalent resistance of the cage, directly increasing the gradient of the torque characteristics in the pull-in region.

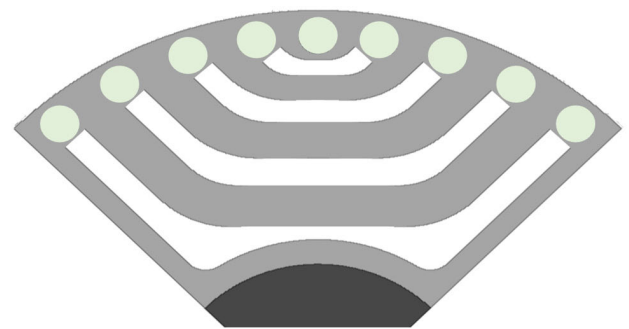


**FIGURE 3.** Proposed LSSynRM rotor: sketch featuring four rectangular flux barriers and symmetric rotor cage based on 36 round rotor slots.

The proper sizing of the trapezoid slot is relevant in achieving good starting performance and high-efficiency steady-state operations. Therefore, strong efforts have been



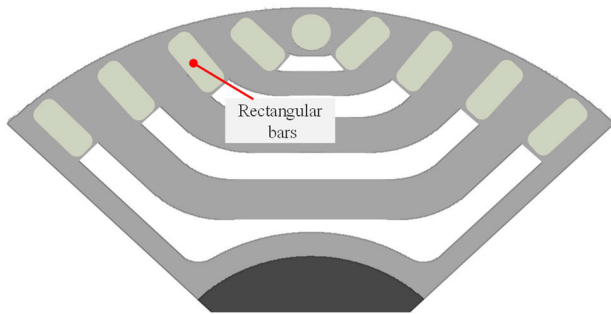


**FIGURE 4.** Proposed LSSynRM rotor: sketch of the rotor with elongated rotor bars in an asymmetric cage layout.

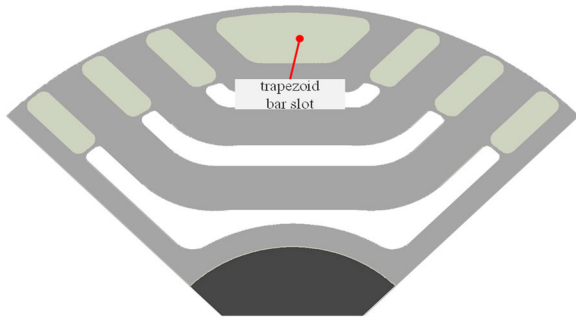


**FIGURE 5.** Proposed LSSynRM rotor: preliminary design of the asymmetric cage featuring rectangular bars and trapezoid bar in the fourth barrier.

dedicated to refining the trapezoid slot by properly size the height and width of the trapezoid bars. Furthermore, the size of the other rectangular bars, and the positioning of the inner ribs have been also refined with respect to the preliminary design.

Detailed investigations on the effects of the torque oscillations at start-up or in steady-state operation have been taken into account in the refining steps [38], [39]; where sensitivity analysis and robust design procedures are suggested to reduce performance variation in series production [40].

The detailed discussion of the refinement and optimization steps is not the paper's purpose, in large part a restricted topic due to IP protection. Nevertheless, the performances of the prototyped motor are extensively discussed in comparison with the reference IE3 IM to demonstrate not only the effectiveness of the proposed design but mainly to demonstrate the validity of the LSSynRM technology in high-efficiency fixed-speed applications.

The refinement and optimization steps result in the rotor for the 4 kW, 4-pole, 400 V, 50 Hz, frame size IEC 112 LSSynRM.

The motor is required to fall into the IE4 efficiency class according to [1]. This implies an efficiency of at least 91.1% (at 50 Hz) without tolerances. The motor is meant to replace the IE3 class IM (efficiency > 88.6 %), achieving a higher efficiency class by applying the proposed low tooling costs approach.

**TABLE 3.** Main data of the LSSynRM final design.

Quantity	Unit	value
Rated power	kW	4
Line voltage and frequency	V, Hz	400, 50
Rated speed	rpm	1500
Rated torque	Nm	25.5
Efficiency class		IE4
Rated efficiency	%	91.1
Critical Inertia vs. rotor inertia ratio		>10
Frame size		IEC 112
Rotor cage		die-cast Al
Stator outer and inner diameter	mm	170, 103
Stack length	mm	160
Airgap	mm	0.30
Number of flux barriers per pole		4
Rotor skew		One slot pitch
Rotor inertia	kgm <sup>2</sup>	105x10 <sup>-4</sup>
Slot fill factor		0.43
Squirrel cage weight	kg	0.93
Total rotor weight (shaft not included)	kg	9.2
Total motor weight (active parts)	kg	26.4
Power vs. weight increase *		14%
Torque vs. volume increase *		13.5%
* only active parts, reference: target IM		

The main data of the final design are reported in Table 3, while the picture of the manufactured rotor core is presented in Fig. 6. The end-ring shape appears the same as the IM one due to the use of the same die-casting mold (end-ring fins are not shown to protect manufacturer IP).

#### IV. LSSynRM: EXPERIMENTAL PERFORMANCE

An extensive test campaign has been carried out on the prototype; the related results are discussed in this session to demonstrate the effectiveness of the proposed technology.

The presented experimental results aim to analyze four main aspects: the steady-state performance, the torque characteristics, the pull-in performance, and the machine behavior in the starting transient.

##### A. STEADY-STATE PERFORMANCE

The steady-state performance aims to mainly demonstrate the efficiency of the prototype at steady-state operation under different loads.

Fig. 7 shows the experimental efficiency curves at different load torques for the IM and the LSSynRM (at 400 V, 50 Hz).

The computation of the loss components has been performed according to Standard IEC 60034-2-1.

The performance of the prototype successfully demonstrates that the LSSynRM efficiency is higher than the limit value for the IE4 class (91.1%): this means that a further material reduction would also be possible.

Moreover, the efficiency of the LSSynRM presents a wide high-efficiency performance varying the load, higher than 90% between the 50% and 150% of the rated load torque.

Adopting the LSSynRM rotor technology reduces the total losses by 27% of the target IM, leading to a steady-state winding temperature rise reduction of about 20 °C. The losses are detailed in Table 4.

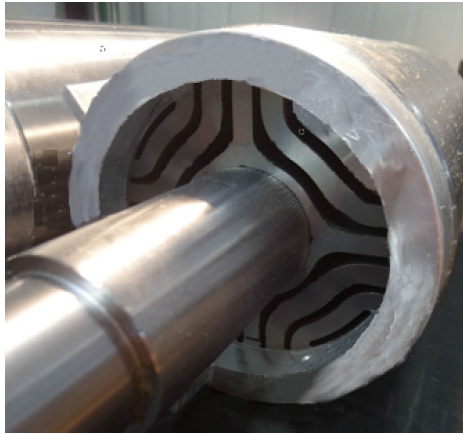


FIGURE 6. View of the rotor of the LSSynRM prototype (end-ring fins removed for confidentiality issues).

The LSSynRM Joule losses in the stator winding are higher because of the higher current and the considerable magnetizing component.

The core losses are lower concerning the IM (−14%), mainly due to the smaller volume of the stator core and the operation at synchronous speed.

The stray-load losses are 28% higher than the ones in the IM. This result can be explained considering that in the LSSynRM, the losses in the cage at steady-state are not null, as the theory would suggest [41]. It can be proved that also at synchronous speed, the cage has eddy currents whose contribution is not effective on the torque performance itself; nonetheless, their presence introduces some additional losses.

The friction and windage (F&W) losses were evaluated at no-load by the indirect method, and the bearings, the fan, and speed are substantially the same in the two cases; then, the amount of such losses is equivalent.

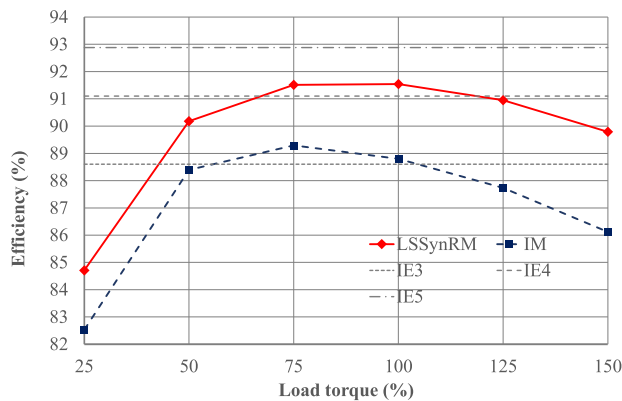


FIGURE 7. Experimental efficiency vs. load torque at 400 V/50 Hz.

The LSSynRM prototype is affected by a weak power factor, reflecting this technology’s main drawback, needing further investigations and research.

TABLE 4. Comparison between the IM and the LSSynRM steady-state performance @ 400 V/50 Hz.

	unit	IM Exp	LSSynRM	
			Exp	Sim
Line voltage	V		400	
Frequency	Hz		50	
Rated power	kW		4	
Stack length	mm	180	160	160
Rated torque $T_n$	Nm	26.4	25.5	25.5
Speed	rpm	1446	1500	1500
Slip		0.036	0	0
Rated current $I_n$	A	7.89	8.69	8.48
Efficiency	%	88.8	91.6	91.4
Total losses	W	503	368	379
Joule Losses	W	186	217	209
Cage losses	W	151	-	-
Core losses	W	125	107	118
Stray-load losses	W	29	37	42
F&W losses	W	12	7	10
Stator temp. rise	°C	52	33	44
Power Factor		0.82	0.72	0.76

\*Experimental (Exp); Simulation (Sim)

TABLE 5. Experimental locked rotor performance of the IM and the LSSynRM @ 400 V/50 Hz.

	unit	IM Experimental	LSSynRM Experimental
Line voltage	V	400	
Frequency	Hz	50	
Locked rotor torque $T_{LR}$	Nm	97	109
$T_{LR} / T_n$		3.7	4.3
Locked rotor current $I_{LR}$	A	67.2	63.7
$I_{LR} / I_n$		8.5	7.3

### B. TORQUE CHARACTERISTICS

Table 5 shows the experimental results of the locked rotor test at 400 V, 50 Hz, and the comparison with the performance of the IE3 class IM.

Since the temperature of the machine affects the locked rotor test, it was performed on the LSSynRM at a temperature close to that of the steady-state (or rather with a stator winding temperature rise of 52 °C and 33 °C for the IM and LSSynRM, respectively). Since the LSSynRM has an asymmetrical cage, the locked rotor torque depends on the rotor position. Thus, the test was repeated several times at different rotor positions, monitoring and keeping constant the temperature during the execution of the various tests. A difference of about 20 Nm was found between the best and the worst result: the value reported in Table 5 refers to the latter. Nonetheless, despite the lower operational temperature, the LSSynRM locked rotor torque is better than the IM one (+12%), with a lower current (−5%).

Table 6 shows the experimental results of the breakdown test. It was performed at the steady-state temperature, gradually increasing the load torque applied to the motor until the loss of synchronism. The prototype is able to maintain the synchronous speed up to twice the rated torque.

**TABLE 6.** Experimental breakdown performance of the LSSynRM @ 400 V/50 Hz.

Quantity	Unit	Value
Line voltage	V	400
Frequency	Hz	50
Breakdown torque $T_{BD}$	Nm	50.5
$T_{BD} / T_n$	-	1.98
Breakdown current $I_{BD}$	A	22.1
$I_{BD} / I_n$	-	2.5

Figure 8 shows the average torque vs. slip characteristics of the IM and the LSSynRM, where the pull-in torque trajectory is reported in the dotted line. The curves were reconstructed according to the results of the previous tests and the controlled braking deceleration test.

The maximum torque of the LSSynRM is very close to the locked rotor torque, and it corresponds to a slip of about 0.7, which is higher than that of the IM (0.37); moreover, the sag of the pull-up torque seems not to be present.

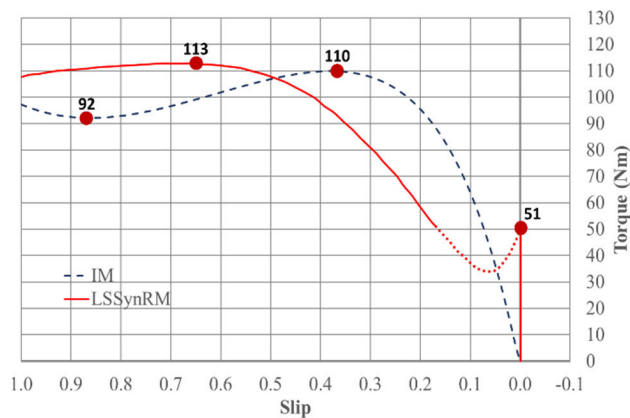


**FIGURE 8.** Reconstructed torque vs. slip characteristics of the LSSynRM and the IM, according to the results of the experimental tests.

**C. PULL-IN PERFORMANCE**

As discussed in Section III, the machine’s starting performance is affected by different aspects. The effects on the starting capability of the load torque, inertia, and motor temperature have been experimentally investigated; the results are discussed in the followings.

The requirement for the design of the LSSynRM in terms of the pull-in capability was to start a load with ten times the rotor’s own inertia ( $105 \times 10^{-4} \text{ kgm}^2$ ) at steady-state temperature and constant load torque equal to the rated one (25.5 Nm).

For this test, a certain number of flywheels were mounted on a dedicated test bench (Fig. 9). In this way, it was possible to study the behaviour of the LSSynRM with different combinations of load torque and inertia.

A high-dynamics test bench based on a PM brushless e-drive was used as a load. It was tuned to achieve a constant braking torque: the delay in reaching the reference torque was

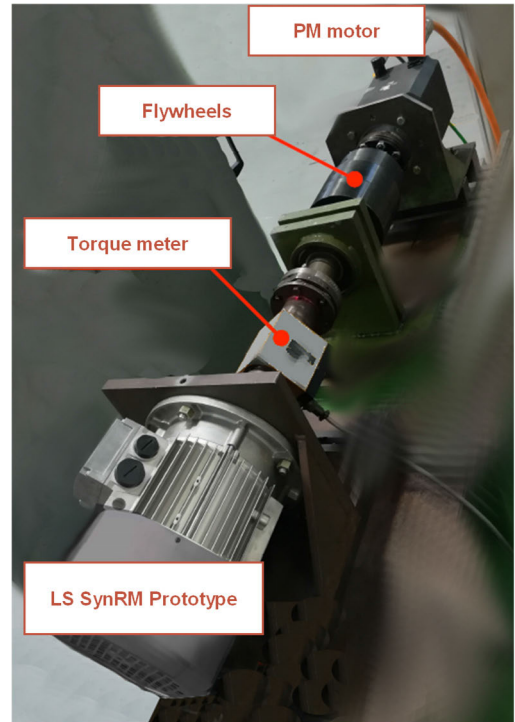


**FIGURE 9.** Test bench for the evaluation of the pull-in performance.

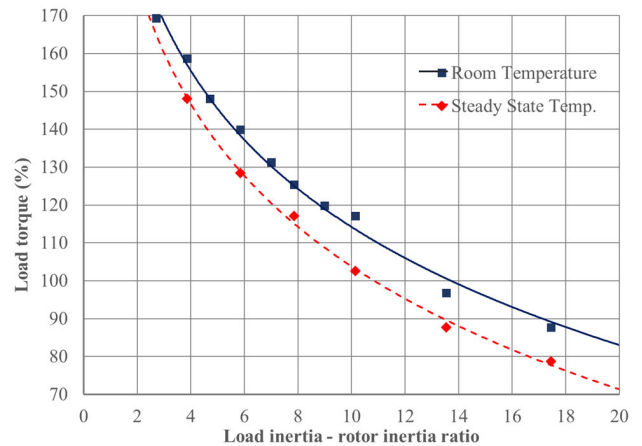


**FIGURE 10.** Pull-in performance: experimental load torque vs. load inertia and rotor inertia ratio: comparison at room and steady-state temperature, rotor inertia  $105 \times 10^{-4} \text{ kgm}^2$ .

less than 10 ms, which can be considered negligible since the overall starting transient is about 0.5s when the machine operates at full load.

The pull-in capability has been validated by two different series of tests. The first series was carried out by maintaining the motor at room temperature (about 20 °C) with a very slow test cycle; the second series was carried out with the prototype pre-heated at the steady-state temperature before each test. Housing temperature and winding resistance were monitored during the tests to maintain as much as possible the same machine temperature in each test series.

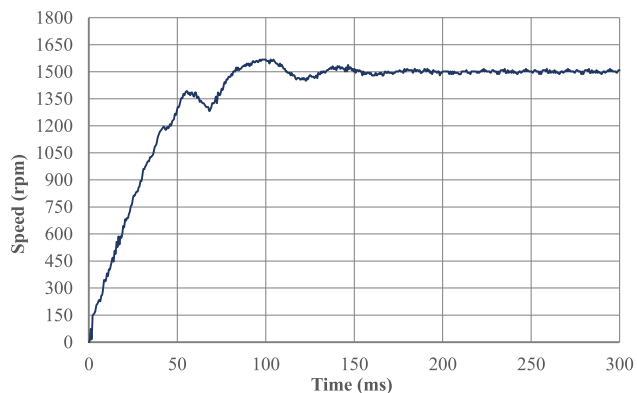


FIGURE 11. Starting transient: experimental speed of the LSSynRM.

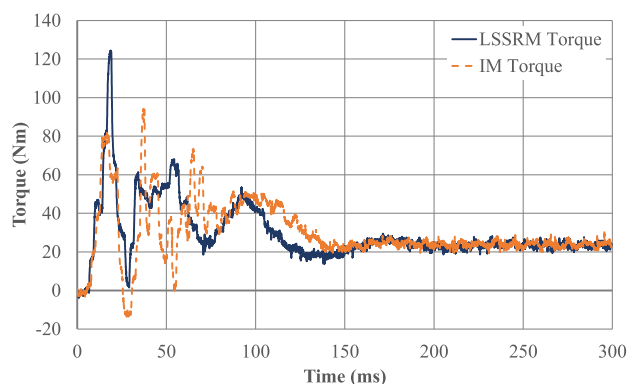


FIGURE 12. Starting transient: experimental torque of the LSSynRM (blue) and the one of the IM (dashed orange).

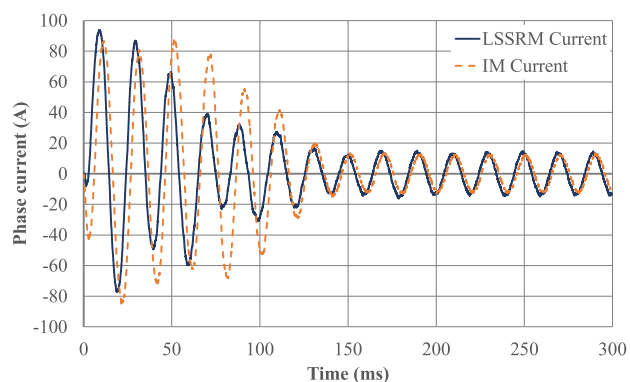


FIGURE 13. Starting transient: phase current of the LSSynRM (blue) and the one of the IM (dashed orange).

Figure 10 shows the pull-in capability in terms of load torque (as a percent of the rated one) vs. the load inertia–rotor inertia ratio at room and steady-state temperature.

The test outcome is positive, showing that the LSSynRM prototype can successfully start a load of almost 11 times the rotor inertia at steady-state temperature when the rated torque is applied. It is worth underlining the effect of temperature in

terms of pull-in capability reduction; it is about  $-20\%$  at rated load torque.

Furthermore, details of the starting operation are reported in Figures 11 to 12. Figure 11 reports the LSSynRM speed during the starting operation up to the pull-in at the synchronous speed. Figure 12 shows the related measured torque; torque pulses affect the motor dynamics and are visible in the speed transients. Nevertheless, excluding the first peak, the torque pulses are equivalent to the IM ones, recorded in the same starting conditions and superimposed in the figure for comparison.

Figure 12 shows the experimental trends of the phase current during the starting transient for the LSSynRM and IM, respectively; the amplitude of the starting current of the LSSynRM is initially slightly higher while decreases with a quicker transient down to the steady-state level.

### V. CONCLUSION

The paper presents design hints, challenges, and opportunities of the line-start synchronous reluctance motor as a high-efficiency alternative to the traditional IM at reduced manufacturing costs. The discussion is supported by experimental investigations on an LSSynRM prototype properly designed to replace a commercial 4 kW, 4-pole, 400 V, 50 Hz, IE3 induction motor.

The main result achieved with the proposed LSSynRM is higher efficiency than the commercial IM with reduced modifications to the manufacturing process; the prototype is manufactured with the same tooling, components, and active materials and can fall entirely into the IE4 efficiency class.

Despite the concerns related to the poor starting performance and the limited pull-in capabilities of the LSSynRM, the tests on the prototype demonstrate that a globally acceptable behavior of the LSSynRM is reachable by proper design. Thus, specific tests concerning the locked rotor torque, the pull-in performance, and the starting transient demonstrate that the LSSynRM can start similar loads of the IM in terms of torque, while applications where the inertia is higher than 10 times the rotor one must be specifically investigated.

The main drawback of this technology seems to be the poor power factor, of minor concern in industrial applications where proper correction systems are often used.

The developed LSSynRM prototype proved a cost-effective, mass production-ready solution for super-premium efficiency IE4 motors. Thanks to its overall performance, LSSynRM can effectively replace the conventional IE3 class IM of the same size in low-inertia applications, i.e. gear motors, belt-driven fans, centrifugal pumps, and centrifugal compressors

In conclusion, LSSynRM is a promising alternative to the IM in a vast panorama of fixed-speed low-inertia industrial applications demanding high efficiency.

Future research will investigate the starting performance in specific medium to high inertia applications where the load torque is not constant.



## REFERENCES

- [1] *Rotating Electrical Machines—Part 30-1: Efficiency Classes of Line Operated AC Motors (IE Code)*, Standard IEC/EN 60034-30-1, International Electrotechnical Commission, 2014.
- [2] A. T. De Almeida, F. J. Ferreira, and J. A. Fong, “Standards for efficiency of electric motors,” *IEEE Ind. Appl. Mag.*, vol. 17, no. 1, pp. 12–19, Jan. 2010.
- [3] A. T. de Almeida, F. J. T. E. Ferreira, and A. Q. Duarte, “Technical and economical considerations on super high-efficiency three-phase motors,” *IEEE Trans. Ind. Appl.*, vol. 50, no. 2, pp. 1274–1285, Mar. 2014.
- [4] A. De Almeida, J. Fong, C. U. Brunner, R. Werle, and M. Van Werkhoven, “New technology trends and policy needs in energy efficient motor systems—A major opportunity for energy and carbon savings,” *Renew. Sustain. Energy Rev.*, vol. 115, Nov. 2019, Art. no. 109384.
- [5] *Rotating Electrical Machines—Part 12: Starting Performance of Single-Speed Three-Phase Cage Induction Motors International Electrotechnical Commission*, Standard IEC/EN 60034-12, 2016.
- [6] A. Hassanpour Isfahani and S. Vaez-Zadeh, “Line start permanent magnet synchronous motors: Challenges and opportunities,” *Energy*, vol. 34, no. 11, pp. 1755–1763, Nov. 2009.
- [7] R. R. Moghaddam and F. Gyllensten, “Novel high-performance SynRM design method: An easy approach for a complicated rototopology,” *IEEE Trans. Ind. Electron.*, vol. 61, no. 9, pp. 5058–5065, Sep. 2014.
- [8] I. Boldea and L. Tutelea, *Reluctance Electric Machines: Design and Control*. Boca Raton, FL, USA: CRC Press, 2019.
- [9] A. Castagnini, H. Kansakangas, J. Kolehmainen, and P. S. Termini, “Analysis of the starting transient of a synchronous reluctance motor for direct-on-line applications,” in *Proc. IEMDC*, Coeur d’Alene, ID, USA, May 2015, pp. 121–126.
- [10] M. Gamba, E. Armando, G. Pellegrino, A. Vagati, B. Janjic, and J. Schaab, “Line-start synchronous reluctance motors: Design guidelines and testing via active inertia emulation,” in *Proc. ECCE*, Montreal, QC, Canada, 2015, pp. 4820–4827.
- [11] J. Tampio, T. Käsäkangas, S. Suuriniemi, J. Kolehmainen, L. Kettunen, and J. Ikaheimo, “Analysis of direct-on-line synchronous reluctance machine start-up using a magnetic field decomposition,” *IEEE Trans. Ind. Appl.*, vol. 53, no. 3, pp. 1852–1859, May/Jun. 2017.
- [12] Y. Hu, B. Chen, Y. Xiao, J. Shi, and L. Li, “Study on the influence of design and optimization of rotor bars on parameters of a line-start synchronous reluctance motor,” *IEEE Trans. Ind. Appl.*, vol. 56, no. 2, pp. 1368–1376, Mar. 2020.
- [13] V. Abramenko, J. Barta, I. Lolova, I. Petrov, and J. Pyrhonen, “Design of a low-power direct-on-line synchronous reluctance motor based on the modified natural flux line curve approach,” *IEEE Trans. Ind. Appl.*, vol. 57, no. 6, pp. 5894–5906, Nov. 2021.
- [14] H. Kim, Y. Park, S.-T. Oh, H. Jang, S.-H. Won, Y.-D. Chun, and J. Lee, “A study on the rotor design of line start synchronous reluctance motor for IE4 efficiency and improving power factor,” *Energies*, vol. 13, no. 21, p. 5774, Nov. 2020.
- [15] F. J. T. E. Ferreira, G. Baoming, and A. T. de Almeida, “Reliability and operation of high-efficiency induction motors,” in *Proc. IEEE/IAS 51st Ind. Commercial Power Syst. Tech. Conf. (I CPS)*, May 2015, pp. 1–13.
- [16] A. Ashwin, M. Dixit, and V. Chavan, “Design optimization of 15 kW, 2-pole induction motor to achieve IE4 efficiency level with copper die-casting,” in *Proc. Int. Conf. Technol. Advancements Power Energy (TAP Energy)*, Jun. 2015, pp. 98–102.
- [17] A. Boglietti, A. Cavagnino, L. Ferraris, M. Lazzari, and G. Luparia, “No tooling cost process for induction motors energy efficiency improvements,” *IEEE Trans. Ind. Appl.*, vol. 41, no. 3, pp. 808–816, May 2005.
- [18] A. Cavagnino, S. Vaschetto, L. Ferraris, Z. Gmyrek, E. B. Agamloh, and G. Bramerdorfer, “Striving for the highest efficiency class with minimal impact for induction motor manufacturers,” *IEEE Trans. Ind. Appl.*, vol. 56, no. 1, pp. 194–204, Feb. 2020.
- [19] A. T. De Almeida, F. J. T. E. Ferreira, and A. Quintino, “Technical and economical considerations on super high-efficiency three-phase motors,” in *Proc. 48th IEEE Ind. Commercial Power Syst. Conf.*, Aug. 2012, pp. 1–13.
- [20] A. de Almeida, F. J. T. E. Ferreira, and J. Fong, “Standards for efficiency of electric motors,” *IEEE Ind. Appl. Mag.*, vol. 17, no. 1, pp. 12–19, Jan./Feb. 2011.
- [21] R. T. Ugale and B. N. Chaudhari, “Rotor configurations for improved starting and synchronous performance of line start permanent-magnet synchronous motor,” *IEEE Trans. Ind. Electron.*, vol. 64, no. 1, pp. 138–148, Jan. 2017.
- [22] D. Mingardi and N. Bianchi, “Line-start PM-assisted synchronous motor design, optimization, and tests,” *IEEE Trans. Ind. Electron.*, vol. 64, no. 12, pp. 9739–9747, Dec. 2017.
- [23] M. Doppelbauer, “Line-start permanent magnet motors and their use in typical industrial applications,” in *Proc. EEMODS*, Rio de Janeiro, Brazil, Aug. 2013, pp. 212–240.
- [24] D. Mingardi, N. Bianchi, and M. D. Prè, “Geometry of line start synchronous motors suitable for various pole combinations,” *IEEE Trans. Ind. Appl.*, vol. 53, no. 5, pp. 4360–4367, Oct. 2017.
- [25] A. Vagati, A. Canova, M. Chiampi, M. Pastorelli, and M. Repetto, “Improvement of synchronous reluctance motor design through finite-element analysis,” in *Proc. Conf. Rec. IEEE Ind. Appl. Conf., 34th IAS Annu. Meeting*, Phoenix, AZ, USA, vol. 2, 1999, pp. 862–871.
- [26] M. Villani, M. Santececca, and F. Parasiliti, “High-efficiency line-start synchronous reluctance motor for fan and pump applications,” in *Proc. ICEM*, Alexandroupoli, Greece, 2018, pp. 2178–2184.
- [27] A. Kersten, Y. Liu, D. Pehrman, and T. Thiringer, “Rotor design of line-start synchronous reluctance machine with round bars,” *IEEE Trans. Ind. Appl.*, vol. 55, no. 4, pp. 3685–3696, Jul. 2019.
- [28] J. F. H. Douglas, “Pull-in criterion for reluctance motors,” *Trans. Amer. Inst. Electr. Eng., II, Appl. Ind.*, vol. 79, no. 3, pp. 139–142, Jul. 1960.
- [29] S. F. Rabbi and M. A. Rahman, “Critical criteria for successful synchronization of line-start IPM motors,” *IEEE J. Emerg. Sel. Topics Power Electron.*, vol. 2, no. 2, pp. 348–358, Jun. 2014.
- [30] M. Palmieri, M. Perta, F. Cupertino, and G. Pellegrino, “Effect of the numbers of slots and barriers on the optimal design of synchronous reluctance machines,” in *Proc. Int. Conf. Optim. Electr. Electron. Equip. (OPTIM)*, May 2014, pp. 1–35.
- [31] G. Pellegrino, F. Cupertino, and C. Gerada, “Automatic design of synchronous reluctance motors focusing on barrier shape optimization,” *IEEE Trans. Ind. Appl.*, vol. 51, no. 2, pp. 1465–1474, Mar./Apr. 2015.
- [32] A. Credo, A. Cristofari, S. Lucidi, F. Rinaldi, F. Romito, M. Santececca, and M. Villani, “Design optimization of synchronous reluctance motor for low torque ripple,” in *A View of Operations Research Applications in Italy (AIRO Springer)*. Cham, Switzerland: Springer, 2019, pp. 53–69.
- [33] H. Kim, Y. Park, S.-T. Oh, G. Jeong, U.-J. Seo, S.-H. Won, and J. Lee, “Study on analysis and design of line-start synchronous reluctance motor considering rotor slot opening and bridges,” *IEEE Trans. Magn.*, vol. 58, no. 2, pp. 1–6, Feb. 2022.
- [34] Y. Hu, B. Chen, Y. Xiao, J. Shi, X. Li, and L. Li, “Rotor design and optimization of a three-phase line-start synchronous reluctance motor,” *IEEE Trans. Ind. Appl.*, vol. 57, no. 2, pp. 1365–1374, Mar. 2021.
- [35] C.-T. Liu, P.-C. Shih, Z.-H. Cai, S.-C. Yen, H.-N. Lin, Y.-W. Hsu, T.-Y. Luo, and S.-Y. Lin, “Rotor conductor arrangement designs of high-efficiency direct-on-line synchronous reluctance motors for metal industry applications,” *IEEE Trans. Ind. Appl.*, vol. 56, no. 4, pp. 4337–4344, Aug. 2020.
- [36] I. Boldea, *Reluctance Synchronous Machines, and Drives*. Oxford, U.K.: Clarendon Press, 1996.
- [37] J. R. Hendershot and T. J. E. Miller, *Design of Brushless Permanent Magnet Machines*. Venice, FL, USA: Motor Design Books LLC, 2010.
- [38] H. L. Garbarino and E. T. B. Gross, “The Goerges phenomenon—Induction motor with unbalanced rotor impedance,” *AIEE Trans.*, vol. 69, pp. 1569–1575, Jan. 1950.
- [39] A. Negahdari and H. A. Toliyat, “Studying crawling effect in line-start synchronous reluctance motors (LS-SynRM),” in *Proc. IEEE 25th Int. Symp. Ind. Electron. (ISIE)*, Santa Clara, CA, USA, Jun. 2016.
- [40] A. Credo, G. Fabri, M. Villani, and M. Popescu, “A robust design methodology for synchronous reluctance motors,” *IEEE Trans. Energy Convers.*, vol. 35, no. 4, pp. 2095–2105, Dec. 2020.
- [41] J. Rituper, J. Gudelhofer, and R. Gottkewaskamp, “Consideration of the skin effect in a transient model of line-start synchronous reluctance machines,” in *Proc. Int. Conf. Electr. Mach. (ICEM)*, Aug. 2020, pp. 1–10.



**MARCO VILLANI** received the M.S. degree in electrical engineering from the University of L’Aquila, L’Aquila, Italy, in 1985. He became an Assistant Professor of power converters, electrical machines, and drives in 1993. In 1990, he was a Research Fellow with the University of Dresden, German, and Nagasaki University, Nagasaki, Japan, in 1995. He is currently an Associate Professor of electrical machines design for the degree of engineering at the University of L’Aquila. His research interests include the modeling and simulation of electrical machines, high-efficiency induction motors, optimization techniques for the electrical machines design, design of PM synchronous motors, and reluctance motors.



**GIUSEPPE FABRI** (Member, IEEE) received the M.S. degree in electronic engineering and the Ph.D. degree in electrical and information engineering from the University of L'Aquila, Italy, in 2009 and 2013, respectively. He is currently an Assistant Professor with the Department of Industrial and Information Engineering and Economics, University of L'Aquila. In 2013, he was a Research Fellow with the Swiss Federal Institute of Technology, Lausanne, Switzerland. His main research

activities concern development, control, and test of electrical motors and drives mainly related to fault-tolerant systems for aircraft and automotive applications. In detail, he has experience in the design of power electronics, DSP-based control platforms, and the implementation of motion control algorithms for ac drives. He designed and tested different development tools, test benches, and demonstrators to aid innovative electric drives' design and validation process.



**LINO DI LEONARDO** was born in Pescara, Italy, in October 1986. He received the M.S. degree in computer and automation engineering and the Ph.D. degree in electrical and information engineering from the University of L'Aquila, in 2010 and 2014, respectively. In particular, his Ph.D. thesis concerns dynamic co-simulation analysis of motor drives. In 2012, he was a visiting Ph.D. student with the École Supérieure d'Ingénieurs en Électrotechnique et Électronique d'Amiens (ESIEE-Amiens). He currently works as an Assistant

Researcher with the Department of Industrial and Information Engineering and Economics, University of L'Aquila. His research activities involve the designing, modeling, and simulation of electrical machines focusing on permanent-magnet synchronous motors, dual-rotor permanent magnet induction machine, and reluctance motors. He has experience with finite-element and multi-physics integrated simulation tools and DSP-based real-time simulation platforms.



**ANDREA CREDO** received the B.Sc. and M.Sc. degrees (Hons.) in electrical engineering and the Ph.D. degree (*cum laude*) from the University of L'Aquila, L'Aquila, Italy, in 2015, 2017, and 2021, respectively. His research interest includes the design and control of synchronous reluctance motors. He received the ICEM Jorma Luomi Student Forum Award during the ICEM 2020, Gothenburg, Sweden (virtual conference).



**FRANCESCO PARASILITI COLLAZZO** received the M.S. degree in electrical engineering from the Sapienza University of Rome, Italy, in 1981. In 1983, he joined the Department of Electrical Engineering, University of L'Aquila, Italy, as an Assistant Professor. From 1992 to 1999, he has been an Associate Professor of electrical drives with the University of L'Aquila. Since 2000, he has been a Full Professor with the University of L'Aquila, where he has been the Head of the

Department of Industrial and Information Engineering and Economics, from 2012 to 2018. His studies deal with the design optimization of induction, PM synchronous and reluctance motors, the modeling and parameter observation of induction and synchronous machines, and the digital control of electrical drives. Since 2004, he has been a member of the Steering Committee of the International Conference on Electrical Machines (ICEM). From 2010 to 2019, he has been the Vice-Chair of the ICEM Steering Committee. He is currently the Chair of the ICEM Administrative Committee (ex-steering committee).

...

Open Access funding provided by 'Università degli Studi dell'Aquila' within the CRUI CARE Agreement